Available online at www.sciencedirect.com
ScienceDirect
Journal of Sound and Vibration 311 (2008) 421–439
JOURNAL OF SOUND AND VIBRATION
www.elsevier.com/locate/jsvi

Probabilistic collocation for period-1 limit cycle oscillations

Jeroen A.S. Witteveen*, Alex Loeven, Sunetra Sarkar, Hester Bijl

Faculty of Aerospace Engineering, Delft University of Technology, Kluyverweg 1, 2629 HS Delft, The Netherlands

Received 16 May 2007; received in revised form 7 September 2007; accepted 18 September 2007
Available online 24 October 2007

Abstract

In this paper probabilistic collocation for limit cycle oscillations (PCLCO) is proposed. Probabilistic collocation (PC) is a non-intrusive approach to compute the polynomial chaos description of uncertainty numerically. Polynomial chaos can require impractical high orders to approximate long-term time integration problems, due to the fast increase of required polynomial chaos order with time. PCLCO is a PC formulation for modeling the long-term stochastic behavior of dynamical systems exhibiting a periodic response, i.e. a limit cycle oscillation (LCO). In the PC method deterministic time series are computed at collocation points in probability space. In PCLCO, PC is applied to a time-independent parametrization of the periodic response of the deterministic solves instead of to the time-dependent functions themselves. Due to the time-independent parametrization the accuracy of PCLCO is independent of time. The approach is applied to period-1 oscillations with one main frequency subject to a random parameter. Numerical results are presented for the harmonic oscillator, a two-dof airfoil flutter model and the fluid-structure interaction of an elastically mounted cylinder.
© 2007 Elsevier Ltd. All rights reserved.

1. Introduction

In the last decades the increase of computer power has resulted in a significant increase of the accuracy of numerical simulations. Compared to the reduced numerical errors, the effects of uncertainty in the input data of the computational analysis are nowadays relatively large. The uncertain input data itself can be obtained as system output response of experiments or preceding analysis. It is important to model these uncertainties to further increase the confidence in numerical predictions. This is especially true for the effects of input uncertainty on the long-term behavior of dynamical systems. It is known that nonlinear dynamical systems can be sensitive to input variability [1]. The amplification of input variability in dynamical systems is of interest to engineers in, for example, flutter analysis.

Parametric uncertainty given by a random variable, which can be described using a polynomial chaos expansion, is considered in this work. This description of uncertainty is relevant in many practical applications involving parametric uncertainty. The polynomial chaos expansion is a polynomial expansion of the response in terms of independent random variables and deterministic coefficients [2,3]. Polynomial chaos is based on the homogeneous chaos theory of Wiener [4]. The deterministic coefficients can be solved for numerically by applying the stochastic Galerkin method [2,5] or the probabilistic collocation (PC) method [6,7].

*Corresponding author.
E-mail address: j.a.s.witteveen@tudelft.nl (J.A.S. Witteveen).

0022-460X/$ - see front matter © 2007 Elsevier Ltd. All rights reserved.
doi:10.1016/j.jsv.2007.09.017

In the stochastic Galerkin method [2,5] the basis polynomials are orthogonal with respect to the input probability density. The Galerkin projection in probability space results in a coupled system of deterministic equations. For Gaussian random variables the stochastic Galerkin method has been developed by Ghanem and Spanos [2]. It has been extended to other standard distributions in the generalized polynomial chaos by Xiu and Karniadakis [3] and arbitrary probability measures [5,8,9]. Multi-element polynomial chaos methods have also been developed [10–12]. Several non-polynomial-based stochastic expansions have also been proposed, e.g. the Wiener–Haar expansion by Le Maître et al. [13] and the Fourier Chaos expansion by Millman et al. [14].

A relatively new method to solve for the polynomial chaos coefficients is the PC method [6,7]. In PC the uncertainty quantification problem is collocated in Gauss points in probability space. The suitable Gauss points are the zeros of polynomials orthogonal with respect to the probability density of the uncertain input. The basis polynomials are the Lagrange polynomials based on the collocation points in probability space. PC leads to a non-intrusive approach in which uncoupled deterministic problems are solved for various parameter values as in Monte Carlo (MC) simulations. It has recently been applied successfully to several problems, see for example [6,7,15–18]. In Ref. [6] exponential convergence of the PC method has been proven under moderate assumptions on the input data. It has also been demonstrated that the PC method can be seen as a generalization of the stochastic Galerkin method [2,5].

The polynomial chaos representation, both in the combination with the stochastic Galerkin method and the PC method, has been applied to several time-dependent problems in [1,19–22]. It has been reported that the polynomial chaos expansion works effectively for many problems, however, it can have difficulty to approximate long-term time integration problems involving random frequencies [21]. In time-dependent problems the required polynomial chaos order to maintain an acceptable accuracy can increase rapidly with time. In a multi-element approaches the same holds for the increase of the number of elements in time [12]. The polynomial chaos description can therefore require an impractical high order to approximate long-term time integration problems. Furthermore, polynomial chaos approximations both in combination with the stochastic Galerkin method and the PC method can fail asymptotically.

The long-term periodic behavior of time-dependent problems is important in the flutter analysis of aeroelastic systems. Flutter is the loss of dynamical stability at a critical dynamic pressure to a time periodic instability that can grow in an unbounded fashion [23]. The instability can lead to catastrophic failure with no periodic motion ever safely reached. Nonlinear systems can exhibit a stable periodic response beyond the flutter point which is known as a limit cycle oscillation (LCO). Here, cases of mild flutter are considered where the limit cycle levels are not destructive. At the flutter point the response usually bifurcates from a damped response to a period-1 oscillation. In practice LCO of aeroelastic systems is of interest to engineers, since it can lead to fatigue failure of the wing structure [14]. It is known that the existence of LCO depends on input variations [20]. The properties of LCO are sensitive to parametric uncertainty [1] in wing structure, store mass and alignment, dynamic pressure, load factors, etc [14]. Therefore, the complete analysis of LCO should include the quantification of the effects of physical input uncertainty.

Although LCO in aeroelastic systems is an active field of research, probabilistic studies of aeroelastic stability are relatively new. Liaw and Yang [24] employed a perturbation approach to examine the aeroelastic behavior of laminated plates and shells subject to structural and geometric uncertainties. Lindsley [25] studied LCO of panels with uncertain modulus of elasticity and thermal expansion coefficient using MC simulation. In Ref. [14] the Fourier chaos expansion is proposed to determine the dynamic response of aeroelastic systems. Wiener–Haar expansions were compared to polynomial chaos expansions for representing the stochastic response of nonlinear aeroelastic systems by Pettit and Beran [20]. They reported that polynomial chaos expansions have difficulty modeling long-term stochastic limit cycle oscillations, because of energy loss after several mean periods of oscillation. The loss of energy remains even for very high-order polynomial chaos expansions, but seems to be less for Wiener–Haar expansions [13,20]. A stall flutter model subject to structural uncertainties is studied in Ref. [26].

Frequency domain methods, e.g. incremental harmonic balance, have been considered for solving linear stochastic operator equations using polynomial chaos expansions [27]. These methods have the advantage that the accuracy of their long-term approximation of periodic solutions can be superior to that of time marching

schemes. The time integration scheme can significantly influence the accuracy of the long-term approximation of stable periodic solutions, as demonstrated in for example [28].

In this paper a PC formulation for modeling the long-term stochastic behavior of LCOs in linear and nonlinear problems is proposed. The idea is to apply PC to a time-independent parametrization of the response instead of to the time-dependent response itself. Due to the time-independent parametrization the accuracy of the PCLCO approximation is independent of time, which enables it to resolve the long-term stochastic behavior of dynamical systems. In practice the error can slightly increase with time due to numerical integration errors. For LCOs a suitable parametrization of the periodic response consists of the frequency, the relative phase, the amplitude, a reference value and the normalized period. A PC approach is employed since it can approximate these functionals of the response more effectively than a stochastic Galerkin method.

The functionals of the response are independent of time, such that the polynomial chaos order of their approximation is time independent, even though a polynomial chaos approximation of the response itself would require a fast increasing order with time. These functionals therefore require a lower order of approximation after sufficiently long-term time integration. Furthermore, these functionals require a relatively low degree, if they are smooth functions of the response. It is demonstrated in the test problems that this can often be the case. In this work, it is assumed that the functionals are smooth functions of the response and that the polynomial approximation of the PC method is appropriate. PCLCO can be seen as an alternative post-processing for PC, since they both employ the same uncoupled deterministic solves at the collocation points in probability space. Research questions about PC itself concerning the global polynomial approximation of non-smooth functionals and the analysis of its numerical errors are outside the scope of this paper. For an error analysis of the PC method is referred to Ref. [6]. It is remarked, however, that by using the non-intrusive PC approach, the polynomial chaos expansion has no influence on the error in the long-term behavior of the deterministic samples.

In flutter analysis one is usually interested in the effect of uncertainty on the bifurcation point from a damped response to a LCO. At the flutter point the damped response often changes to a period-1 oscillation with one main frequency. An initial quantification of the effect of uncertainty usually focuses on the effect of individual parameters. The application of the current formulation of PCLCO is therefore limited to period-1 LCOs with one main frequency subject to one uncertain parameter. It is assumed that these oscillations exist in the relevant parameter domain. The extension of the approach to more complex dynamical systems needs further attention.

In practical applications it might not be trivial to ensure *a priori* that periodic solutions exist for the relevant input parameter range. It is therefore determined *a posteriori* whether the deterministic samples are periodic. The response is considered to be periodic, if after sufficiently long integration time, $t_{\max}$, the response results within a threshold value in identical orbits in phase-space. The effect of the threshold on the approximation with PCLCO at $t_{\max}$ is small, since the parametrization is extracted from the last full period before $t_{\max}$. If all samples have a periodic response, then PCLCO post-processing is applied to the samples. Otherwise normal PC post-processing applied, since both PCLCO and PC are based on the same deterministic samples.

A harmonic oscillator problem with an uncertain spring stiffness is considered to demonstrate that PCLCO is able of capturing the long-term stochastic behavior of LCOs successfully. This model problem, which is similar to the sinusoidal model problem studied by Pettit and Beran [20], does not involve a transient part in the deterministic response. An error convergence study up to a polynomial chaos order of 8 is performed. Subsequently, PCLCO is applied to other engineering applications involving periodic response. A two-dof airfoil flutter model is considered subject to uncertainty in the structure. This problem is used to study the effect of a deterministic transient behavior on the PCLCO approach. Finally, a combination of PCLCO and PC is employed to propagate the uncertainty through a fluid-structure interaction simulation of an elastically mounted cylinder with an uncertain free stream velocity. In that case, PC is applied for short-term integration in the transient part of the deterministic time series. The stochastic transient behavior and the long-term stochastic response are resolved using PCLCO.

The PC approach for LCOs is introduced in Section 2. Numerical results are presented for the harmonic oscillator, the airfoil flutter model and the elastically mounted cylinder in Section 3. The paper is concluded in Section 4.

2. Probabilistic collocation for limit cycle oscillations

In this section, the PC method for LCOs is introduced. It is based on the time-independent parameterization of LCOs given in Section 2.2. First the general PC framework is briefly reviewed in Section 2.1.

2.1. Probabilistic collocation method

PC is based on collocating the stochastic problem in Gauss quadrature points in the probability space [6,7]. Suitable Gauss points are the zeros of polynomials orthogonal with respect to the probability density of the uncertain input. The stochastic moments of the output are computed by Gauss quadrature based on a polynomial approximation of the response and a polynomial chaos description of the probability distribution.

A differential equation is considered subject to parametric input uncertainty with a probabilistic description:

$$\mathscr{L}(a)u = 0, \tag{1}$$

with operator $\mathscr{L}$ in domain $D \subset \mathbb{R}^d \times T$, $d = \{1,2,3\}$, $T = [0, t_{\max}]$ and uncertain input parameter $a(\omega)$ with $\omega \in \Omega$. The set of outcomes of the probability space $(\Omega, \mathscr{F}, P)$ is denoted by Ω, $\mathscr{F} \subset 2^{\Omega}$ is the σ-algebra of events and P is a probability measure. The uncertain variable $u(x,t,\omega)$, with $x \in \mathbb{R}^d$ and $t \in T$, is then approximated in the PC method as

$$u(x,t,\omega) = \sum_{k=1}^{N} u_k(x,t) l_k(a(\omega)), \tag{2}$$

where N is the number of collocation points $\{a_k\}_{k=1}^N$ in probability space and $N-1$ is the polynomial chaos order of approximation (2). The collocation points $\{a_k\}_{k=1}^N$ are the zeros of the polynomial $\pi_{N+1}(a)$, where $\{\pi_i(a)\}_{i=0}^{N+1}$ is the set of polynomials up to order $N+1$ orthogonal with respect to the probability density function $p_a(a)$ of the uncertain input parameter $a(\omega)$. The polynomials $\{\pi_i(a)\}_{i=0}^{N+1}$ are given by the orthogonality relation

$$\langle \pi_i(a)\pi_j(a) \rangle = \int \pi_i(a)\pi_j(a)p_a(a)\,\mathrm{d}a = \langle \pi_i(a)^2 \rangle \delta_{ij}, \tag{3}$$

for $i,j = 1,\ldots,N+1$, where $\langle . \rangle$ denotes an inner product. For several standard input distributions the polynomials $\{\pi_i(a)\}_{i=0}^{N+1}$ in Eq. (3) are (scaled) classical polynomials [29] of which the roots are tabulated to full accuracy. For other input distributions the collocation points can be computed numerically [7].

The deterministic coefficients $\{u_k(x,t)\}_{k=1}^N$ in Eq. (2) are then the deterministic solutions of Eq. (1) for the parameter values $\{a_k\}_{k=1}^N$. The basis polynomials $\{l_k(a)\}_{k=1}^N$ of expansion (2) are Lagrange polynomials with respect to the collocation points $\{a_k\}_{k=1}^N$ for which holds

$$l_k(a_j) = \delta_{jk}, \quad j,k = 1,\ldots,N, \tag{4}$$

where δ_{jk} is the Kronecker delta. The mean $\mu_u(x,t)$ and variance $\sigma_u^2(x,t)$ of the solution $u(x,t,\omega)$ are computed using Gauss quadrature integration based on the quadrature points $\{a_k\}_{k=1}^N$, for example,

$$\mu_u(x,t) = \sum_{k=1}^{N} w_k u_k(x,t), \tag{5}$$

where w_k are Gauss quadrature weights. Multidimensional collocation points can be obtained from tensor products of the one-dimensional collocation points or a sparse grid approach [18].

2.2. Time-independent parametrization of limit cycle oscillations

In long-term time integration of unsteady problems subject to uncertainty the uncertainty response surface $u(x,t,\omega)$ can be a highly nonlinear function of the uncertain input parameter $a(\omega)$ [20]. In that case, the global polynomial representation in the polynomial chaos description is not adequate for approximating the response

surface. Increasing the polynomial chaos order in PC or the number of elements in the multielement generalized polynomial chaos extends the valid integration time [12]. However, the polynomial chaos approximation fails asymptotically due to the growing nonlinearity of the response surface in time.

The long-term periodic response $u(x,t,\omega)$ can be parametrized by a vector of time-independent parameters $z(x,\omega)$ than time t. For a periodic response $z(x,\omega)$ can consist of the frequency, the relative phase, the amplitude, a reference value and the normalized period. This results in a time-independent parametrization of the periodic response $u_{\text{periodic}}(x,z(x,\omega),\omega)$. PC can then be applied to the parametrization $z(x,\omega)$ instead of the time-dependent response $u(x,t,\omega)$ itself. The realizations of the parametrization $z_k(x,\omega)$ are extracted from the same time series $u_k(x,t,\omega)$ as in PC obtained from solving Eq. (1) at the collocation points $\{a_k\}_{k=1}^N$. This enables the use of existing deterministic time integration solvers. The accuracy of the polynomial chaos approximation of the parametrization $z(x,\omega)$:

$$z(x,\omega)=\sum_{k=1}^{N} z_k(x)l_k(a(\omega)) \tag{6}$$

is then independent of time t. If the parametrization $z(x,\omega)$ depends not too nonlinearly on the uncertain input parameter $a(\omega)$, the polynomial chaos order of the approximation of the long-term behavior can be relatively low. The PCLCO approximation of the response $u(x,t,\omega)$ is given by substitution of (6) into a parametrized description of the response. This formulation of PC for LCOs is capable of resolving the effect of the uncertain input parameter $a(\omega)$ on the long-term stochastic response.

As mentioned before, a suitable time-independent parametrization of the asymptotic periodic response of LCOs is a parametrization in terms of the frequency $f(x,\omega)$, the relative phase $\phi(x,\omega)$, the amplitude $A(x,\omega)$, a reference value $u_0(x,\omega)$ and the normalized period $u_{\text{period}}(x,\tau,\omega)$, with $\tau\in[0,2\pi]$. The time series $u_k(x,t,\omega)$ for the N collocation points $\{a_k\}_{k=1}^N$ in probability space result in N realizations of the frequency $f_k(x)$, the phase $\phi_k(x)$, the amplitude $A_k(x)$, the reference value $u_{0_k}(x)$ and the normalized period $u_{\text{period}_k}(x,\tau)$ of the periodic response:

- the frequency $f_k(x)$ is defined as the inverse of the period length, which is the smallest time $t_{\text{period}_k}(x)>0$ for which holds in the asymptotic region $u_k(x,t+t_{\text{period}_k}(x))=u_k(x,t)$;
- The relative phase $\phi_k(x)$ of the time series is defined as the phase of the oscillation at $t=t_{\max}$ with respect to the time of the latest maximum $t_{u_{\max_k}}(x)$ by $\phi_k(x)=n_{\text{periods}_k}(x)+(t_{\max}-t_{u_{\max_k}}(x))f_k(x)$ with $n_{\text{periods}_k}(x)$ the integer number of completed cycles;
- The amplitude $A_k(x)$ is equal to half the difference between the minimum and the maximum of the period $A_k(x)=\frac{1}{2}(u_{\max_k}(x)-u_{\min_k}(x))$;
- the reference value $u_{0_k}(x)$ is chosen to be the average of the minimum and maximum of the period $u_{0_k}=\frac{1}{2}(u_{\min_k}(x)+u_{\max_k}(x))$.

This parametrization is obtained from the last full period of the simulation after establishing a sufficiently long-integration time for the development of the periodic oscillation, see Fig. 1. The polynomial chaos approximation of the parametrization $f(x,\omega)$, $\phi(x,\omega)$, $A(x,\omega)$ and $u_0(x,\omega)$ is then determined using Eq. (6). The PCLCO approximation of the response is given by substituting Eq. (6) into the parametrized description of the response given by

$$u(x,t,\omega)=u_0(x,\omega)+A(x,\omega)u_{\text{period}}(x,\tau(x,\omega),\omega) \tag{7}$$

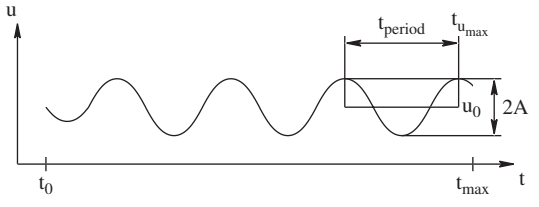

Fig. 1. Definition of parameters to describe limit cycle oscillation in PCLCO.

with $\tau(x,\omega) = 2\pi(\phi(x,\omega) + (t - t_{\max})f(x,\omega)) \pmod{2\pi}$. This results in a non-polynomial response surface approximation. For this expression also an expansion of the normalized period $u_{\text{period}}(x,\tau,\omega)$ similar to Eq. (6) is required. The shape of the period of the deterministic time series $u'_{\text{period}_k}(x,t'_k(x))$ with $t'_k(x) = [0, t_{\text{period}_k}(x)]$ is extracted from the last full period of the functions $u_k(x,t)$. The normalized period $u_{\text{period}_k}(x,\tau)$, with $\tau \in [0,2\pi]$, is obtained by scaling the periods $u'_{\text{period}_k}(x,t'_k(x))$ by their frequency $f_k(x)$, amplitude $A_k(x)$ and equilibrium $u_{0_k}(x)$

$$u_{\text{period}_k}(x,\tau) = \frac{1}{A_k(x)}\left(u'_{\text{period}_k}\left(x, \frac{\tau}{2\pi f_k(x)}\right) - u_{0_k}(x)\right) \tag{8}$$

with $k = 1,\ldots,N$ and $\tau \in [0,2\pi]$. The polynomial chaos approximation of $u_{\text{period}}(x,\tau,\omega)$ based on the representations $u_{\text{period}_k}(x,\tau)$ is given by

$$u_{\text{period}}(x,\tau,\omega) = \sum_{k=1}^{N} u_{\text{period}_k}(x,\tau) l_k(a(\omega)). \tag{9}$$

In practice $u_{\text{period}}(x,\tau,\omega)$ is determined at n_τ discrete angles $\{\tau_j\}_{j=1}^{n_\tau} \in [0,2\pi]$ and interpolation can be employed to obtain $u_{\text{period}}(x,\tau,\omega)$ from $\{u_{\text{period}}(x,\tau_j,\omega)\}_{j=1}^{n_\tau}$. One could also use a Fourier transform to discretize the normalized period. In pseudo-algorithmic form PCLCO can be represented as follows:

(1) solve N deterministic problems for the parameter values corresponding to the N collocation points in probability space;
(2) extract $f_k(x)$, $\phi_k(x)$, $A_k(x)$, $u_{0_k}(x)$, and $u_{\text{period}_k}(x,\tau)$ for $k = 1,\ldots,N$ from the N deterministic solutions;
(3) construct the global polynomial approximations $f(x,\omega)$, $\phi(x,\omega)$, $A(x,\omega)$, $u_0(x,\omega)$, and $u_{\text{period}}(x,\tau,\omega)$ using (6) and (9);
(4) substitute $f(x,\omega)$, $\phi(x,\omega)$, $A(x,\omega)$, $u_0(x,\omega)$, and $u_{\text{period}}(x,\tau,\omega)$ into (7)to find the approximation of the response $u(x,t,\omega)$.

The mean and variance of the response $u(x,t,\omega)$ are determined by numerically integrating of the response surface (7). The distribution function is given by sorting the function u–ω, with $\omega \in [0,1]$, to a monotonically increasing reconstruction.

3. Numerical results

In this section numerical results of PCLCO are presented for the analytical harmonic oscillator problem, a two-degrees-of-freedom airfoil flutter model and a fluid-structure interaction simulation of an elastically mounted cylinder. The results are compared to those of PC see Section 2.1, and MC simulations.

3.1. Harmonic oscillator

The analytical harmonic oscillator problem with an uncertain spring stiffness is considered to demonstrate the properties of PCLCO for a problem with no transient part in the deterministic response. PCLCO is compared to PC in an error convergence study with respect to an MC reference solution. The motion of the harmonic oscillator is described by

$$m\frac{\partial^2 x(t,\omega)}{\partial t^2} + k(\omega)x(t,\omega) = 0, \quad t \in [0,\infty), \tag{10}$$

with deterministic initial conditions $x(0) = \tilde{x}_0 = 1$ and $(\partial x/\partial t)(0) = \tilde{x}_1 = 1$, mass $m = 1$ and uncertain spring stiffness $k(\omega)$ with a lognormal distribution with mean $\mu_k = 1$ and coefficient of variation $\text{CV}_k = 10\%$. The analytical solution of Eq. (10) can be written as

$$x(t,\omega) = x_0(\omega) + A(\omega)\cos(2\pi f(\omega)t + \phi(\omega)), \tag{11}$$

with frequency $f(\omega) = (1/2\pi)\sqrt{k(\omega)/m}$, phase $\tan\phi = \tilde{x}_1/\tilde{x}_0\sqrt{k/m}$, amplitude $A = \tilde{x}_0/\cos\phi$ and reference value $x_0(\omega) = 0$. The response $x(t,\omega)$ given by Eq. (11) is a periodic function of time with no transient part. The solution is considered until $t_{\max} = 100$ which corresponds to approximately 16 periods for μ_k.

PCLCO is employed with three collocation points $\{k_i\}_{i=1}^N$, with $N=3$, for the uncertain parameter $k(\omega)$. The time series $x_i(t)$ are parametrized by f_i, ϕ_i, A_i and x_{0_i}. For this simple model problem the scaled periodic motion $x_{\text{period}}(\tau,\omega)$ is independent of ω since $x_{\text{period}}(\tau,\omega)=\cos(\tau)$ with $\tau\in[0,2\pi]$. The parametrization describes the time series $x_i(t)$ for $t>0$ exactly.

In Fig. 2 the three samples $\{x_i(t)\}_{i=1}^N$ are shown. The periodic responses start at the deterministic initial condition without transient behavior. The uncertainty affects the amplitude and the frequency of the response α. The effect on the frequency results in an increasing phase difference between the time series. The functions diverge from each other in time, since the frequency and amplitude of the time series depend on the sample value k_i.

The mean $\mu_x(t)$ and the variance $\sigma_x^2(t)$ of the response $x(t,\omega)$ are shown in Fig. 3 as function of time t. The approximations of PCLCO and PC for $N=3$ are compared to a MC simulation with 1000 uniformly distributed samples. In contrast to the periodic deterministic solutions, the MC solution for the mean $\mu_x(t)$ is a damped oscillation, see Fig. 3a. The decaying oscillation is caused by the effect of the uncertainty on the

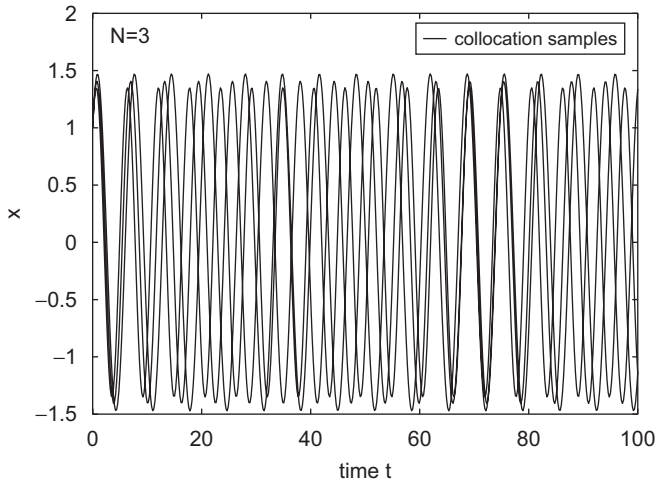

Fig. 2. The three-deterministic realizations at the collocation points for the harmonic oscillator.

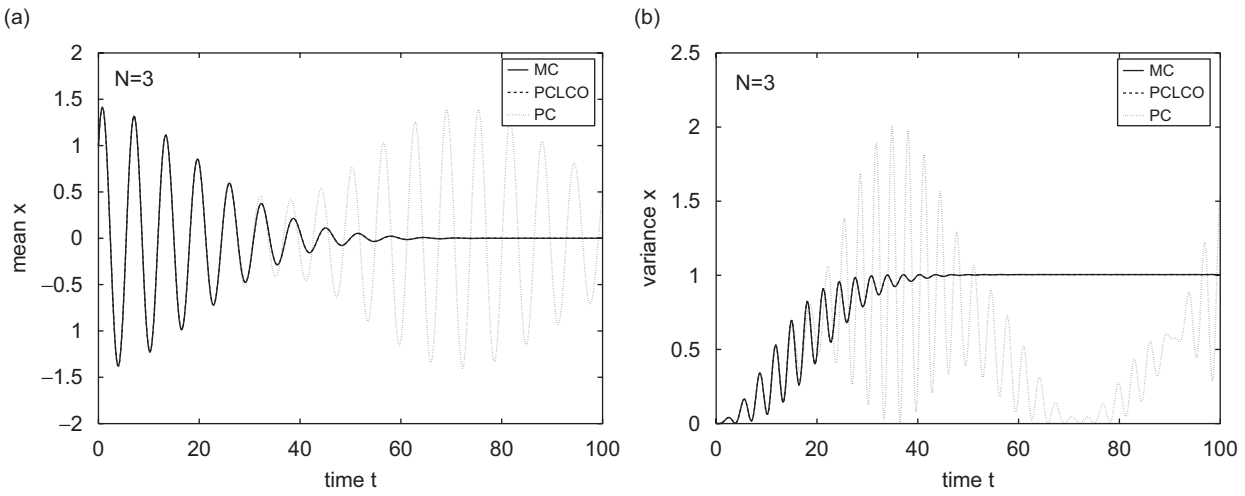

Fig. 3. Response of the harmonic oscillator by Monte Carlo (MC), PCLCO and probabilistic collocation (PC): (a) mean and (b) variance.

frequency of the time series. Due to the increasing phase difference in time, time series with opposite signs increasingly cancel each other.

The result of PCLCO is indistinguishable from the MC result for all times $t \in [0, t_{\max}]$. The PC approximation of the mean is accurate up to approximately $t = 25$. For later times the error of the PC approximation rises to unacceptable levels. Using a higher polynomial chaos order or a multielement approach elongates the domain in which the approximation is accurate. However, without continuously increasing the order the approximation would fail asymptotically for long-term integration at some t [20,21].

The variance $\sigma_x^2(t)$ shows a transient oscillatory behavior until it damps to the steady value of $\sigma_x^2(t) = 1.0$ for $t > 50$, see Fig. 3b. Although the samples shown in Fig. 2 do not exhibit transient behavior and are unsteady for all t, the *stochastic* solution has a transient behavior due to the deterministic initial condition and reaches a steady solution for long-term integration. PCLCO resolves both the transient and the asymptotic stochastic solution as the results of MC and PCLCO are indistinguishable also for the variance. The accuracy of PC deteriorates for the variance at approximately $t = 15$ which is earlier than for the mean. PC is unable to predict the asymptotic steady solution of the variance which results in large errors.

The reason that PCLCO accurately approximates the long-term stochastic behavior already with $N = 3$ is that in PCLCO the polynomial approximation of PC is not applied to the response in terms of the time series $x_i(t)$ directly, but to the parametrization f_i, ϕ_i and A_i. This parametrization of the periodic response is independent of time which enables for an approximation of the asymptotic behavior. In addition, the parametrization $f(\omega)$, $\phi(\omega)$ and $A(\omega)$ depends almost linearly on the uncertain input parameter $k(\omega)$ which results in an accurate approximation with $N = 3$.

In Fig. 4 the approximation of the frequency $f(\omega)$ is given in terms of its response surface with respect to $k(\omega)$ and its probability distribution function. The comparison of the PCLCO approximation and the MC results in Fig. 4a shows that the frequency $f(\omega)$ depends almost linearly on $k(\omega)$. The polynomial PCLCO approximation based on the collocation points results for $N = 3$ in an adequate approximation of the frequency response surface. Therefore, also the probability distribution function of the frequency is accurately resolved, see Fig. 4b. Similar results are obtained for the phase $\phi(\omega)$ and amplitude $A(\omega)$.

Based on the time-independent approximations of $f(\omega)$, $\phi(\omega)$, and $A(\omega)$, the analytical solution (11) gives the time-dependent approximation of $x(t, \omega)$. In Fig. 5 the approximations of the response surface $x(t, \omega)$–$k(\omega)$ and the probability distribution of $x(t, \omega)$ are given for $t = \{1, 20, 100\}$ for MC, PCLCO and PC. The response surface is almost linear after short-term integration, see Fig. 5a. For this case both PCLCO and PC result in accurate approximations of the response surface at $t = 1$. This time interval corresponds to approximately 0.16 periods for μ_k. The approximation of the probability distribution of $x(t, \omega)$ at $t = 1$ is also accurate in Fig. 5b.

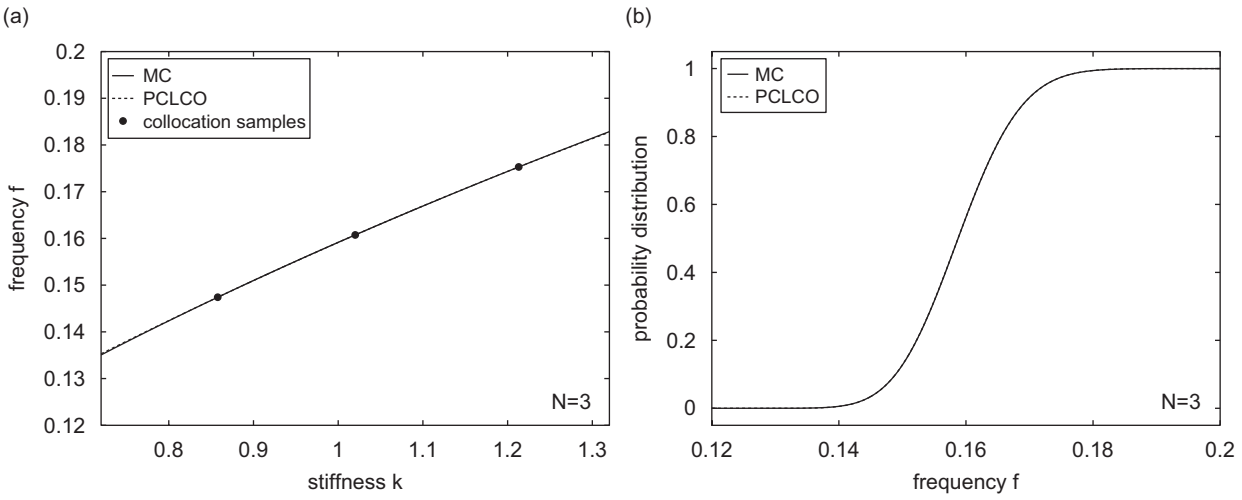

Fig. 4. Frequency of the harmonic oscillator by Monte Carlo (MC) and PCLCO: (a) response surface and (b) probability distribution.

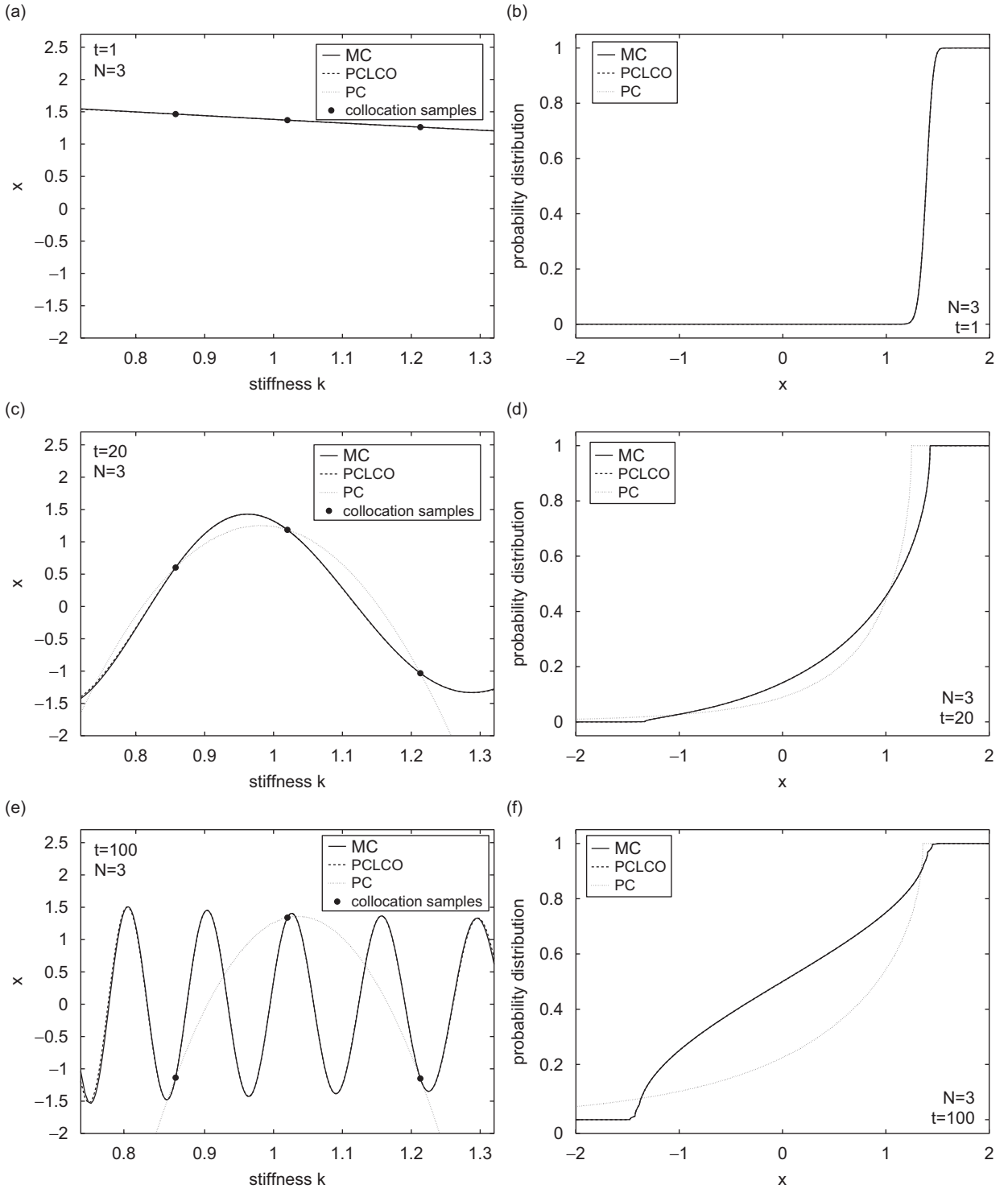

Fig. 5. Response surface $x(t,\omega)$–$k(\omega)$ and its probability distribution by Monte Carlo (MC), PCLCO and probabilistic collocation (PC) for the harmonic oscillator: (a,b) at $t = 1$; (c,d) at $t = 20$; and (e,f) at $t = 100$.

After long-term integration the response surface is increasingly nonlinear, see Figs. 5c and e for the results at $t = 20$ and 100, which corresponds to approximately 3.2 and 16 periods for μ_k, respectively. The PCLCO approximation based on the three collocation points and the parametrization (11) maintains a similar accuracy in the approximation of the response surface independent of the time t. The polynomial approximation of PC through the three collocation points is clearly not adequate to represent the increasingly nonlinear response surface. In Figs. 5d and f the probability distribution of $x(t,\omega)$ after long-term integration is shown for $t = 20$ and 100. The probability distribution function reaches a steady solution asymptotically. PCLCO resolves the detailed features of the probability distribution function also near $x = \pm 0.5$ for all times $t \in [0, t_{\max}]$.

An error convergence study is performed to compare the accuracy of PCLCO and PC for a range of polynomial chaos orders up to $N = 9$ at different times t, see Fig. 6. The convergence study focuses on the contribution of the polynomial chaos expansion to the error in the long-term behavior of the stochastic system, since in this analytical test problem numerical time integration errors are absent. The time-averaged L_1-errors in the approximation of the mean and the variance in different time intervals are considered. In Fig. 6a the error convergence of PCLCO and PC up to $t = 1$ is shown for the error in the mean $\mu_x(t)$. PC results for this short-term integration problem in fast exponential convergence which reaches machine precision for $N = 7$. PCLCO convergences three orders of magnitude to an error lower than 10^{-6} at $N = 9$.

In Fig. 6c the error convergence for the mean at $t = 20$ is shown. PCLCO convergences again to an error lower than 10^{-6} for $N = 9$. PC convergences significantly slower than for the $t = 1$ case to an error of 10^{-3}, which is higher than for PCLCO. This is also demonstrated by the error convergence of the mean for $t = 100$ in Fig. 6e, for which PC hardly convergences, but PCLCO still convergences beyond an error of 10^{-6} for $N = 9$. In Figs. 6b, d and f similar results are shown for the error in the approximation of the variance at $t = 1$, 20, and 100.

To demonstrate that the accuracy of PCLCO is nearly independent of time, the errors in the approximation of the mean and the variance of PCLCO and PC are given as function of time in Fig. 7 for $N = 1$, 5, and 9. For $N = 1$ both PCLCO and PC reduce to a deterministic solve for the mean value of the uncertain input parameter μ_k. For higher polynomial chaos orders $N = 5$ and 9 PCLCO results in a error which is nearly constant in time and decreases for increasing N. The error in the approximation of the variance even decreases with time for short-term integration $t < 20$, see Fig. 7b. The accuracy of PC depends strongly on time. For long-term integration the error in the PC approximation even increases with an increasing polynomial chaos order. The post-processing of the samples is in PCLCO computationally more intensive than in PC. However, the computational costs in engineering applications are dominated by computing the deterministic samples. The number of samples in the PCLCO computation is over a factor 10^2 smaller than in the MC simulation.

3.2. 2 dof flutter model

In this section PCLCO is applied to a relevant model for flutter analysis. Flutter models are often used instead of full unsteady fluid-structure interaction simulations. Here a two-dof model for the pitch and plunge motion of an airfoil, see Fig. 8, is used which was studied deterministically for example by Lee et al. [30] and stochastically using Fourier chaos by Millman et al. [14]. The aeroelastic equations of motion with cubic restoring springs in both pitch and plunge are given in Ref. [30] as

$$\xi'' + x_\alpha \alpha'' + 2\zeta_\xi \frac{\bar{\omega}}{U^*}\xi' + \left(\frac{\bar{\omega}}{U^*}\right)^2 (\xi + \beta_\xi \xi^3) = -\frac{1}{\pi\mu} C_L(\tau), \tag{12}$$

$$\frac{x_\alpha}{r_\alpha^2}\xi'' + \alpha'' + 2\frac{\zeta_\alpha}{U^*}\alpha' + \frac{1}{U^{*2}}(\alpha + \beta_\alpha \alpha^3) = \frac{2}{\pi\mu r_\alpha^2} C_M(\tau), \tag{13}$$

where α is the pitch angle, $\xi = h/b$ is the non-dimensional plunge displacement of the elastic axis, with $b = c/2$ the half-chord, β_ξ and β_α are the nonlinear spring constants, r_α is the radius of gyration about the elastic axis, and ζ_ξ and ζ_α are the viscous damping coefficients in plunge and pitch, respectively. The ratio of natural frequencies is $\bar{\omega} = \omega_\xi/\omega_\alpha$, where ω_ξ and ω_α are the natural frequencies of the uncoupled plunging and pitching modes, respectively. The bifurcation parameter is defined as $U^* = U/(b\omega_\alpha)$. The non-dimensionalized time is

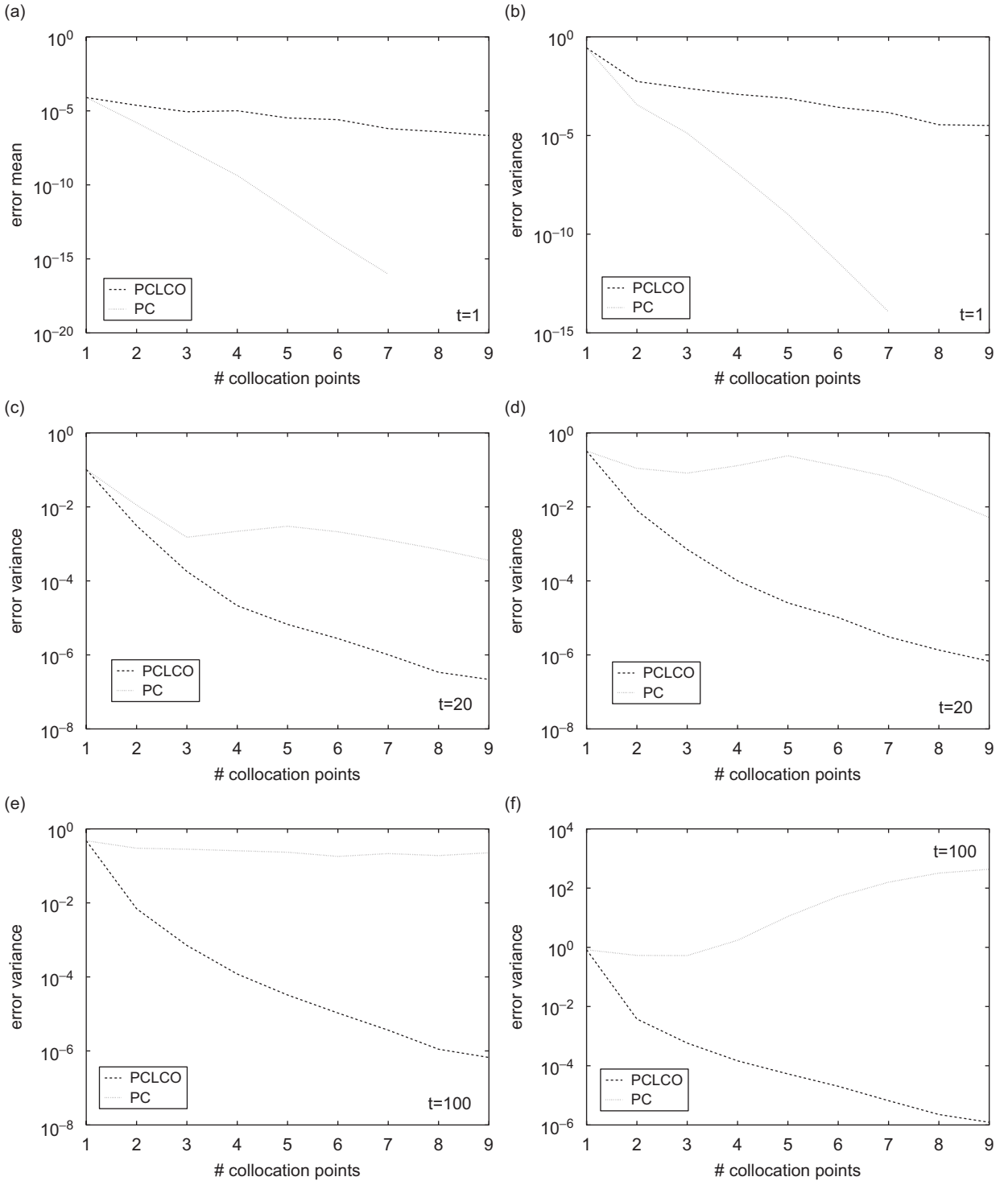

Fig. 6. Error convergence of PCLCO and probabilistic collocation (PC) for the mean and variance for the harmonic oscillator: (a,b) at $t = 1$; (c,d) at $t = 20$; and (e,f) at $t = 100$.

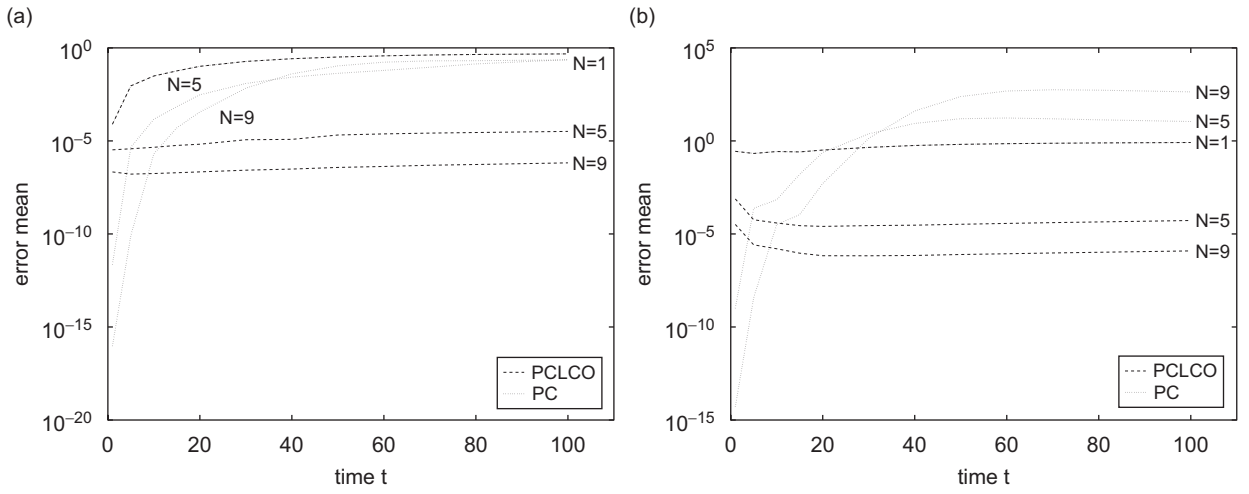

Fig. 7. Error of PCLCO and probabilistic collocation (PC) as function of time for the harmonic oscillator: (a) mean and (b) variance.

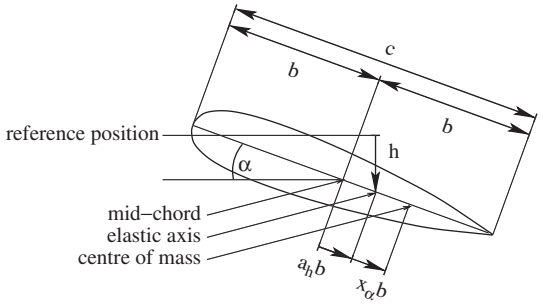

Fig. 8. The two-dof airfoil flutter model.

$\tau = Ut/b$. The expressions for the aerodynamic force and moment coefficients, $C_L(\tau)$ and $C_M(\tau)$ are given by Fung [23] as

$$C_L(\tau) = \pi(\xi'' - a_h\alpha'' + \alpha') + 2\pi\left\{\alpha(0) + \xi'(0) + \left[\frac{1}{2} - a_h\right]\alpha'(0)\right\}\phi(\tau) + 2\pi\int_0^\tau \phi(\tau-\sigma)\left[\alpha'(\sigma) + \xi''(\sigma) + \left(\frac{1}{2} - a_h\right)\alpha''(\sigma)\right]\mathrm{d}\sigma, \tag{14}$$

$$C_M(\tau) = \pi\left(\frac{1}{2} + a_h\right)\left\{\alpha(0) + \xi'(0) + \left(\frac{1}{2} - a_h\right)\alpha'(0)\right\}\phi(\tau) + \pi\left(\frac{1}{2} + a_h\right)\int_0^\tau \phi(\tau-\sigma)\left\{\alpha'(\sigma) + \xi''(\sigma) + \left(\frac{1}{2} - a_h\right)\alpha''(\sigma)\right\}\mathrm{d}\sigma + \frac{\pi}{2}a_h(\xi'' - a_h\alpha'') - \left(\frac{1}{2} - a_h\right)\frac{\pi}{2}\alpha' - \frac{\pi}{16}\alpha'', \tag{15}$$

where the elastic axis is located at a distance $a_h b$ from mid-chord, the mass center is located at a distance $x_\alpha b$ from the elastic axis and $\phi(\tau)$ is the Wagner function

$$\phi(\tau) = 1 - \psi_1 \mathrm{e}^{-\varepsilon_1\tau} - \psi_2 \mathrm{e}^{-\varepsilon_2\tau}, \tag{16}$$

with the constants $\psi_1 = 0.165$, $\psi_2 = 0.335$, $\varepsilon_1 = 0.0455$ and $\varepsilon_2 = 0.3$ given by Jones [31]. Based on Eqs. (12)–(16), a set of first-order ordinary differential equations for the motion of the airfoil is derived in

Ref. [30]. Following Refs. [14,30], these equations are integrated numerically until $\tau = 2000$ using the explicit fourth-order Runge–Kutta method with a time step of $\Delta\tau = 0.1$, which is approximately $1/256$ of the smallest period.

The following parameter values are used: $\mu = 100$, $a_h = -0.5$, $x_\alpha = 0.25$, $r_\alpha = 0.5$ and $\zeta_\alpha = \zeta_\xi = 0$, as in Refs. [14,30]. For a hard spring model in the pitch dof ($\beta_\alpha > 0$) the system exhibits a LCO [32]. The nonlinear torsional spring stiffness parameter is set to $\beta_\alpha = 3$. The ratio of uncoupled plunging and pitching modes natural frequencies $\bar{\omega}$ is assumed to be uncertain described by a lognormal distribution. The mean value $\mu_{\bar{\omega}} = 0.2$ is chosen to be equal to the deterministic value used in Refs. [14,30] with a coefficient of variation of $\mathrm{CV}_{\bar{\omega}} = 10\%$. The effect of the input uncertainty on the mean and variance of the pitch angle $\alpha(\omega)$ and its bifurcation plot is considered. Results for the plunge deflection $\zeta(\omega)$ are qualitatively similar.

The bifurcation parameter U^* is set to 6.6 as in Ref. [14]. PCLCO is applied with $N = 3$ and the results are compared to those of PC, and MC based on 1000 uniformly sampled realizations. To cancel the effect of the finite number of MC samples, the mean and variance of PCLCO and PC are determined based on the same sampling in their response surface approximation as MC. The collocation samples of PCLCO are shown in Fig. 9. The samples show a periodic response with a transient behavior for $\tau < 100$. The uncertainty in $\bar{\omega}$ affects the frequency and the amplitude of the samples. The periodic reconstruction of the time series samples by PCLCO, see (7), is given by the dashed lines. The periodic oscillations for $\tau > 100$ are exactly represented. The transient behavior of the samples for $\tau < 100$ is not modeled in the periodic reconstruction.

In Fig. 10 the mean pitch angle $\mu_\alpha(\tau)$ is given. It shows a transient behavior for $\tau < 100$ after which the mean develops a decaying oscillation. PCLCO results in an excellent match of the long-term MC results. The mean for $\tau < 100$ is not accurately resolved by PCLCO, since it does not model the transient part of the deterministic samples. PC gives an accurate approximation of the mean for $\tau < 800$. For higher values of the non-dimensional time τ, PC does not predict the asymptotic damped oscillation.

The variance of the pitch angle $\sigma_\alpha^2(\tau)$ is given in Fig. 11. The variance is an oscillating increasing function of τ until $\tau \approx 1000$ at which it reaches a steady asymptotic value of approximately $\sigma_\alpha^2 = 1.96 \times 10^{-2}$. PCLCO gives an accurate approximation of the steady behavior for $\tau > 1000$. The transient behavior of the variance for $\tau \in [100, 1000]$ is also accurately resolved, since the *stochastic* transient behavior is due to the deterministic initial condition and not due to the transient behavior of the deterministic samples. The variance for $\tau < 100$ for which the deterministic samples are in their transient is not accurately resolved by PCLCO. However, the transient of the deterministic samples takes less than one-tenth of the stochastic transient part. PC does give an accurate approximation for $\tau < 100$, but it fails for long-term integration for $\tau > 500$.

So, PCLCO and PC seem complementary, where a PC post-processing should be used for the initial time interval in which the deterministic samples exhibit transient behavior. To the long-term periodic behavior of

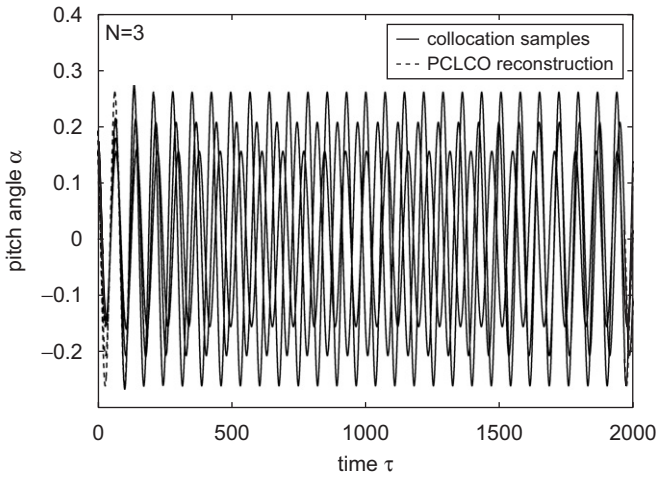

Fig. 9. The three deterministic realizations and their PCLCO reconstruction at the collocation points for the airfoil flutter model.

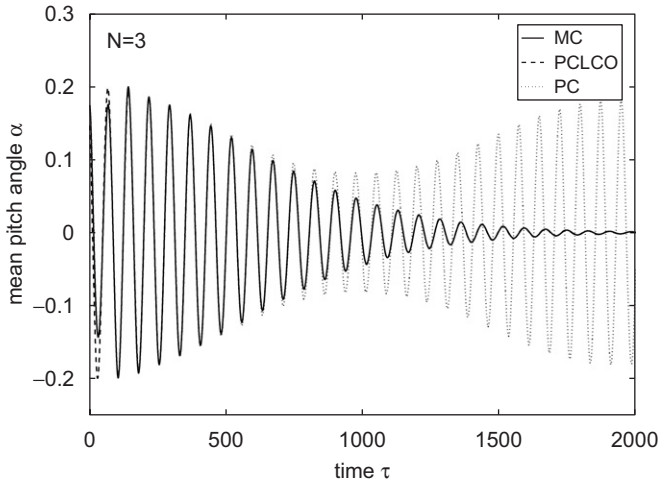

Fig. 10. Mean pitch angle by Monte Carlo (MC), PCLCO and probabilistic collocation (PC) for the two-dof airfoil flutter model.

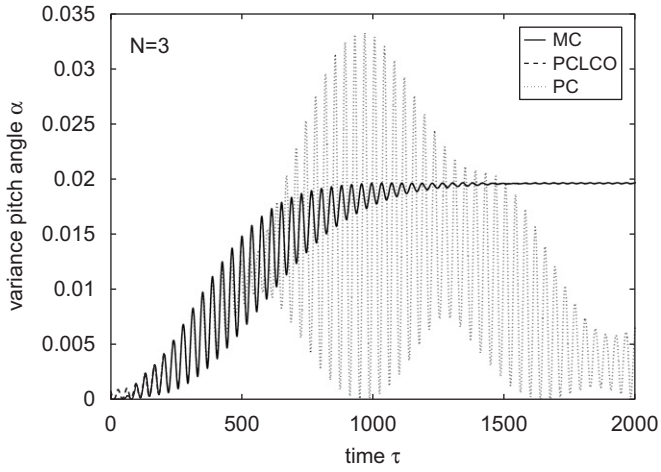

Fig. 11. Variance of the pitch angle by Monte Carlo (MC), PCLCO and probabilistic collocation (PC) for the two-dof airfoil flutter model.

the deterministic samples after their transient, PCLCO post-processing should be applied. This combined approach is demonstrated in the next test problem.

In Fig. 12 the stochastic bifurcation plot of the pitch angle $\alpha(t,\omega)$ is given in terms of the amplitude $A_\alpha(\omega)$ at $\tau = 2000$ with U^* as bifurcation parameter and $\bar{\omega}$ uncertain. The PCLCO approximation of the mean amplitude μ_{A_α} and uncertainty bars based on the 90% confidence interval are shown. The results are compared to the deterministic bifurcation plot for $\bar{\omega} = \mu_{\bar{\omega}}$. The stochastic bifurcation plot is shown in this way, since it is of practical interest to visualize the distortion of the deterministic bifurcation as a result of the input uncertainty. A supercritical Hopf bifurcation [33] is observed in the deterministic bifurcation plot between $U^* = 6.2$ and 6.3, which is the transition of a damped solution to a limit cycle oscillation. The damped oscillation of the response $\alpha(t,\omega)$ below the bifurcation point results in very small amplitudes at $\tau = 2000$.

The interpretation of the bifurcation of the stochastic system is more complex in terms of D-bifurcation and P-bifurcation [34,35]. D- or dynamical-bifurcation is concerned with the loss of stability of an equilibrium point at a qualitative change of its eigenvalues or largest Lyapunov exponent. Phenomenological- or

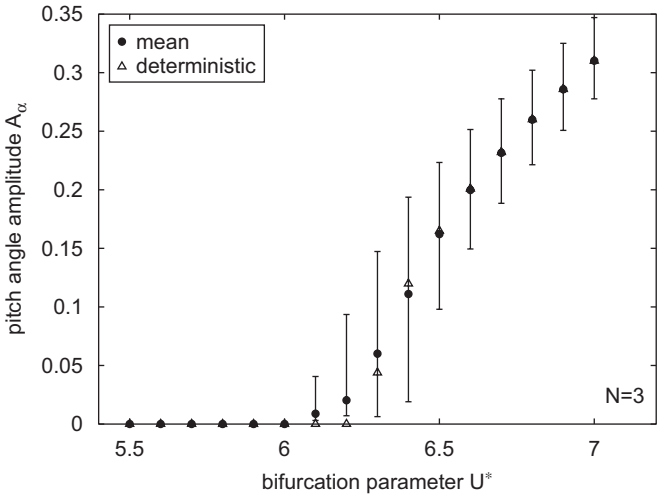

Fig. 12. Stochastic bifurcation plot of the pitch angle amplitude A_α with the mean and 90% uncertainty bars compared to the deterministic case as function of the bifurcation parameter U^*.

P-bifurcation is associated with a qualitative change in the output probability distribution. For a deterministic system the D- and P-bifurcation point coincide.

The stochastic problem is here solved using PCLCO based on $N = 3$ samples, $\bar{\omega}_i = \{0.172; 0.204; 0.243\}$, and a global polynomial interpolation of the response. Near the bifurcation point the true response surface contains a discontinuity in the first derivative. This kink is not resolved as a discontinuity by the global polynomial approximation. Near the bifurcation point the method gives approximate results, which capture the qualitative bifurcation behavior correctly.

The mean of the amplitude $A_\alpha(\omega)$ and the 90% scatter given in Fig. 12 are functionals of probability space. The bifurcation behavior of these functionals appears to be consistent with a deterministic bifurcation. Below $U^* = 6.0$ PCLCO resolves that both the mean and the 90% interval vanish. The uncertainty in the ratio of natural frequencies $\bar{\omega}$ has no effect on the pre-bifurcation amplitudes $A_\alpha(\omega)$.

Between $U^* = 6.0$ and 6.1, one of the three time-series $\alpha(t, \bar{\omega}_3)$, for the sample $\bar{\omega}_3 = 0.243$, bifurcates from a damped oscillation to a LCO. This results in a bifurcation in the mean and the 90% interval between $U^* = 6.0$ and 6.1. The uncertainty in $\bar{\omega}$ has reduced the flutter point from $U^* \in [6.2; 6.3]$ in the deterministic case to $U^* \in [6.0; 6.1]$. For $U^* > 6.1$ the amount of uncertainty in $A_\alpha(\omega)$ increases rapidly until it starts to decrease at $U^* = 6.4$ to an uncertainty bar with a length of approximately 0.07 for $U^* > 6.8$. The mean value μ_{A_α} differs significantly from the deterministic case in the domain $U^* \in [6.0, 6.5]$ around the deterministic bifurcation point.

In addition to the bifurcation of the mean and the 90% interval, the probability density function (PDF) of the amplitude $A_\alpha(\omega)$ exhibits a P-bifurcation. Because near the bifurcation point the approach gives qualitively correct answers, the qualitative P-bifurcation behavior of the PDF of $A_\alpha(\omega)$ is described below. Below $U^* = 6.0$ the PDF is a delta function in the origin. After the bifurcation point of $\alpha(t, \bar{\omega}_3)$ in $U^* \in [6.0; 6.1]$ the PDF has a maximum in the origin and decays monotonically for larger $A_\alpha(\omega)$. This P-bifurcation point coincides with the bifurcation of the mean of $A_\alpha(\omega)$ and the 90% interval. The PDF shows a bell-shape with a maximum at a positive $A_\alpha(\omega)$ value after the bifurcation of the second sample $\alpha(t, \bar{\omega}_2)$, with $\bar{\omega}_2 = 0.204$, in $U^* \in [6.2; 6.3]$.

3.3. Flow past an elastically mounted cylinder

The two-dimensional fluid-structure interaction problem of an elastically mounted circular cylinder in a laminar Navier–Stokes flow is considered in this section, see Fig. 13. The gas flow around the cylinder with

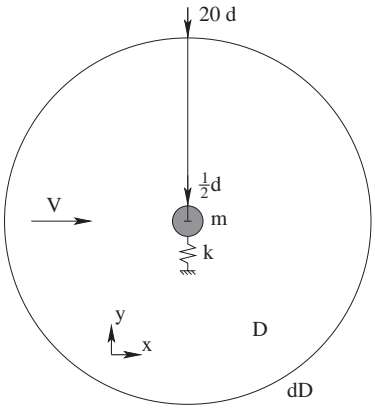

Fig. 13. The elastically mounted cylinder in a uniform free stream flow.

diameter d is governed by the two-dimensional compressible Navier–Stokes equations [36]:

$$\frac{\partial \rho}{\partial t}+\frac{\partial \rho u}{\partial x}+\frac{\partial \rho v}{\partial y}=0, \tag{17}$$

$$\rho\frac{\mathrm{D}u}{\mathrm{D}t}=-\frac{\partial p}{\partial x}+\frac{\partial \tau_{xy}}{\partial y}, \tag{18}$$

$$\rho\frac{\mathrm{D}v}{\mathrm{D}t}=-\frac{\partial p}{\partial y}+\frac{\partial \tau_{xy}}{\partial x}, \tag{19}$$

$$\rho\frac{\mathrm{D}E}{\mathrm{D}t}=\frac{\partial}{\partial x}\left(k\frac{\partial T}{\partial x}\right)+\frac{\partial}{\partial y}\left(k\frac{\partial T}{\partial y}\right)-\frac{\partial pu}{\partial x}-\frac{\partial pv}{\partial y}+\frac{\partial \tau_{xy}v}{\partial x}+\frac{\partial \tau_{xy}u}{\partial y} \tag{20}$$

with density ρ, velocity components u and v in the x-direction and y-direction, respectively, static pressure p, total energy E, Newtonian viscous stress $\tau_{xy}=\mu(\partial v/\partial x+\partial u/\partial y)$, dynamic viscosity μ, and thermal conductivity k. The ideal gas equation of state is given by $p=\rho RT$, with specific gas constant R. The cylinder is only free to move in the cross flow y-direction. The structural stiffness is modeled by a linear spring:

$$\frac{\partial^2 y_{\mathrm{cyl}}}{\partial t^2}+\omega_n^2 y_{\mathrm{cyl}}=F_y(t), \tag{21}$$

where $y_{\mathrm{cyl}}(t,\omega)$ is the y-position of the center of the cylinder, $\omega_n=\sqrt{0.1}\approx 0.316$ is the angular natural frequency of the structure, and $F_y(t)$ is the y-component of the resulting pressure force of the flow onto the structure given by

$$F_y(t)=-\int_{\partial D_{\mathrm{cyl}}} p(x,y,t)\mathbf{n}_{\mathrm{cyl}}\cdot\mathbf{e}_y\,\mathrm{d}s, \tag{22}$$

with $\mathbf{n}_{\mathrm{cyl}}$ the outward pointing normal of the cylinder surface $\partial D_{\mathrm{cyl}}$ and $\mathbf{e}_y$ the unit vector in the y-direction.

The field Eqs. (17)–(20) are discretized on a circular spatial domain D with diameter $40d$ using a second-order finite volume method on a grid of 1.2×10^4 volumes. An arbitrary Lagrangian–Eulerian formulation is employed to couple the fluid mesh with the movement of the structure. Time integration is performed using a BDF-2 method with a stepsize of $\Delta t=0.25$ until $t=250$. The boundary conditions on the surface of the cylinder $\partial D_{\mathrm{cyl}}$ are $u=0$ and $v=\partial y_{\mathrm{cyl}}/\partial t$. The uniform undisturbed flow conditions $u=V$ and $v=0$ are imposed on the outer boundary of the fluid domain ∂D. Initially, the flow field is uniform and the cylinder is at rest with an initial deflection of $y_{\mathrm{cyl}}=0.5d$ with respect to its equilibrium position.

The undisturbed velocity in the x-direction, V, is assumed to be uncertain described by a truncated lognormal distribution with a coefficient of variation of $\mathrm{CV}_V=10\%$. The mean value of the velocity $\mu_V=0.3$

corresponds to a Reynolds number of $Re = 1000$. The truncated lognormal distribution limits the variation of the Reynolds number to the range for which the frequency of the periodic fluid motion is typically given by a Strouhal number of $\mathrm{St} = fd/V = 0.2$. This corresponds for μ_V to an angular frequency of $\omega_{\mathrm{flow}} = 0.38$. For this range the cylinder exhibits a period-1 oscillation. The variation in V affects the frequency of the vortex pattern behind the cylinder and, therefore, influences the frequency of the motion of the cylinder.

A combination of PCLCO and PC is used to solve for the stochastic response of the cylinder in the whole-time domain. For the short-term integration in the transient part of the deterministic time series PC is applied. PCLCO is employed for resolving the stochastic transient behavior and the long-term stochastic response. In Figs. 14 and 15 the evolution of the mean and the variance of the cylinder displacement $y(t, \omega)$ is shown. To demonstrate the convergence of the combined approach for short-term and long-term integration, the approximations for $N = 2$ to 4 are shown. PC is applied to the deterministic samples in an initial time interval starting at $t = 0$. From the time where the PCLCO and PC approximations match, the PCLCO approach is applied. These points are in Figs. 14 and 15 denoted by the symbols.

A similar behavior of the mean and the variance can be seen as for the previous test problem. The mean is a decaying oscillation after the transient part of the deterministic solves, see Fig. 14. The variance approaches an

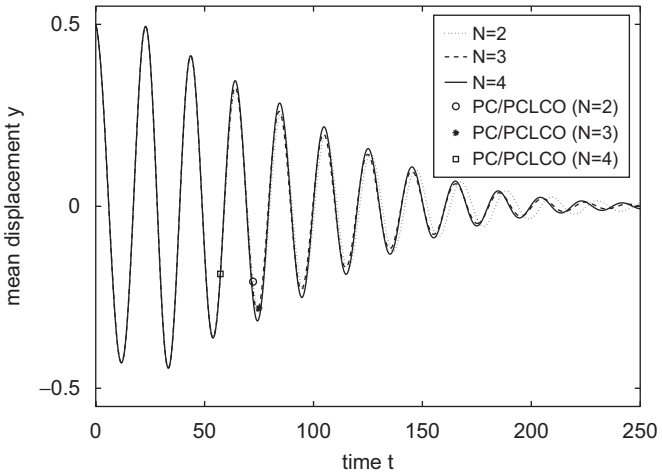

Fig. 14. Mean deflection of the elastically mounted cylinder for the combination of PCLCO and probabilistic collocation (PC).

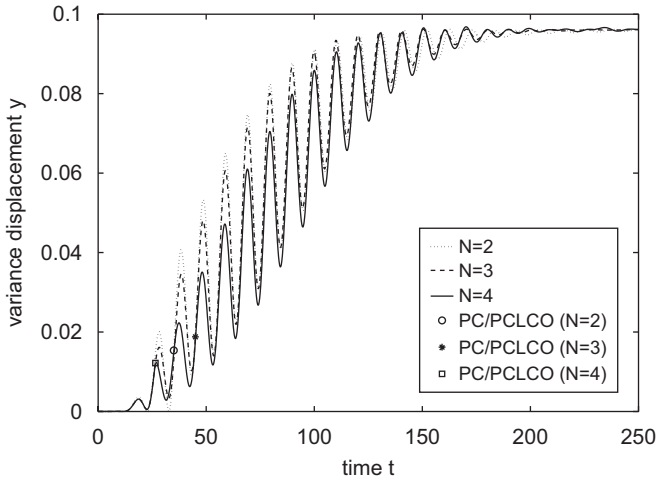

Fig. 15. Variance of the deflection of the elastically mounted cylinder for the combination of PCLCO and probabilistic collocation (PC).

asymptotic value of approximately 9.6×10^{-2} after an oscillatory stochastic transient, which extends beyond the deterministic transient, see Fig. 15.

In the initial time interval PC gives a converged solution already for the low order approximations, which is demonstrated by the coinciding approximations for $N = \{2, 3, 4\}$. PCLCO also shows a converging solution, especially for the long term integration results $t > 150$. In the stochastic transient $t \in [50, 150]$ the results of PCLCO seem to converge less rapidly.

4. Conclusions

A PC formulation for modeling the long-term stochastic behavior of LCOs is proposed. In PCLCO, PC is applied to a time-independent parametrization of the periodic time series at the collocation points in probability space. Due to its independence of time the PCLCO approximation is capable of modeling the long-term stochastic behavior of dynamic systems. For LCO a suitable parametrization of the periodic deterministic solutions consists of the frequency, relative phase, amplitude, reference value and normalized period. PCLCO is applied to period-1 oscillations with one main frequency subject to an uncertain parameter. Numerical results are presented for the harmonic oscillator, an airfoil flutter model and the flow around an elastically mounted cylinder.

It has been demonstrated that standard polynomial chaos computed using PC is initially accurate, but that it is unable to predict the long-term stochastic behavior as its accuracy depends strongly on time. PCLCO accurately predicts the long-term stochastic response and the *stochastic* transient solution caused by deterministic initial conditions. The accuracy of the PCLCO approximation of the mean and the variance is shown to be independent of time. In practice, the error can slightly increase with time due to numerical integration errors. PCLCO does however not resolve the stochastic solution in the transient part of the deterministic response, since it does reconstruct the periodic behavior of the collocation samples. PCLCO and PC therefore seem complementary, where PC should be used to model the stochastic response for the initial time interval in which the deterministic functions are in their transient part. For resolving the long-term stochastic solution after the transient behavior of the deterministic samples, PCLCO should be employed. Further testing of the method with actually measured data scatter is recommended to evaluate its properties in, for example, the aeronautical application of flutter suppression in wing structures. The extension of the method beyond the current assumptions requires further attention.

Acknowledgments

This research was supported by the Technology Foundation STW, applied science division of NWO and the technology programme of the Ministry of Economic Affairs.

References

[1] C.L. Pettit, P.S. Beran, Effects of parametric uncertainty on airfoil limit cycle oscillations, *Journal of Aircraft* 40 (5) (2004) 1217–1229.
[2] R.G. Ghanem, P.D. Spanos, *Stochastic Finite Elements: A Spectral Approach*, Springer, New York, 1991.
[3] D.B. Xiu, G.E. Karniadakis, The Wiener-Askey polynomial chaos for stochastic differential equations, *SIAM Journal of Scientific Computing* 24 (2) (2002) 619–644.
[4] N. Wiener, The homogeneous chaos, *American Journal of Mathematics* 60 (1938) 897–936.
[5] I. Babuška, R. Tempone, G.E. Zouraris, Galerkin finite element approximations of stochastic elliptic partial differential equations, *SIAM Journal of Numerical Analysis* 42 (2) (2004) 800–825.
[6] I. Babuška, F. Nobile, R. Tempone, A stochastic collocation method for elliptic partial differential equations with random input data, *SIAM Journal of Numerical Analysis* 45 (3) (2007) 1005–1034.
[7] G.J.A. Loeven, J.A.S. Witteveen, H. Bijl, Probabilistic collocation: an efficient non-intrusive approach for arbitrarily distributed parametric uncertainties, *45th AIAA Aerospace Sciences Meeting and Exhibit*, Reno, NV, 2007, AIAA-2007-317.
[8] X.L. Wan, G.E. Karniadakis, Multi-element generalized polynomial chaos for arbitrary probability measures, *SIAM Journal of Scientific Computing* 28 (3) (2006) 901–928.
[9] J.A.S. Witteveen, H. Bijl, Modeling arbitrary uncertainties using Gram–Schmidt polynomial chaos, *44th AIAA Aerospace Sciences Meeting and Exhibit*, Reno, NV, 2006, AIAA-2006-896.

[10] M. Deb, I. Babuška, J. Oden, Solution of stochastic partial differential equations using Galerkin finite element techniques, *Computer Methods in Applied Mechanics and Engineering* 190 (2001) 6359–6372.
[11] O.P. Le Maître, H.N. Najm, R.G. Ghanem, O.M. Knio, Multi-resolution analysis of Wiener-type uncertainty propagation schemes, *Journal of Computational Physics* 197 (2004) 502–531.
[12] X.L. Wan, G.E. Karniadakis, An adaptive multi-element generalized polynomial chaos method for stochastic differential equations, *Journal of Computational Physics* 209 (2) (2005) 617–642.
[13] O.P. Le Maître, O.M. Knio, H.N. Najm, R.G. Ghanem, Uncertainty propagation using Wiener–Haar expansions, *Journal of Computational Physics* 197 (2004) 28–57.
[14] D.R. Millman, P.I. King, P.S. Beran, A stochastic approach for predicting bifurcation of a pitch and plunge airfoil, *21th AIAA Applied Aerodynamics Conference*, Orlando, FL, 2003, AIAA-2003-3515.
[15] G. Lin, C.-H. Su, G.E. Karniadakis, Modeling uncertainties in supersonic flow past a wedge, *44th AIAA Aerospace Sciences Meeting and Exhibit*, Reno, NV, 2006, AIAA-2006-0124.
[16] L. Mathelin, M.Y. Hussaini, Th.A. Zang, Stochastic approaches to uncertainty quantification in CFD simulations, *Numerical Algorithms* 38 (1–3) (2005) 209–236.
[17] M.A. Tatang, Direct Incorporation of Uncertainty in Chemical and Environmental Engineering Systems, PhD Thesis, MIT, Cambridge, 1995.
[18] D.B. Xiu, J.S. Hesthaven, High-order collocation methods for differential equations with random inputs, *SIAM Journal of Scientific Computing* 27 (3) (2005) 1118–1139.
[19] D. Lucor, G.E. Karniadakis, Noisy inflows cause a shedding-mode switching in flow past an oscillating cylinder, *Physical Review Letters* 9215 (15) (2004) 4501.
[20] C.L. Pettit, P.S. Beran, Spectral and multiresolution Wiener expansions of oscillatory stochastic processes, *Journal of Sound and Vibration* 294 (2006) 752–779.
[21] X.L. Wan, G.E. Karniadakis, Long-term behavior of polynomial chaos in stochastic flow simulations, *Computational Methods in Applied Mathematics* 195 (2006) 5582–5596.
[22] D.B. Xiu, G.E. Karniadakis, Modeling uncertainty in flow simulations via generalized polynomial chaos, *Journal of Computational Physics* 187 (2003) 137–167.
[23] Y. Fung, *An Introduction to Aeroelasticity*, Dover Publications, New York, 1969.
[24] D.G. Liaw, H.T.Y. Yang, Reliability and nonlinear supersonic flutter of uncertain laminated plates, *AIAA Journal* 31 (12) (1993) 2304–2311.
[25] N.J. Lindsley, P.S. Beran, C.L. Pettit, Effects of uncertainty on nonlinear plate aeroelastic response, *43rd AIAA/ASME/ASCE/AHS/ASC Structures, Structural Dynamics, and Materials Conference*, Denver, CO, 2002, AIAA-2002-1271.
[26] J.A.S. Witteveen, S. Sarkar, H. Bijl, Modeling physical uncertainties in dynamic stall induced fluid-structure interaction of turbine blades using arbitrary polynomial chaos, *Computers & Structures* 85 (2007) 866–878.
[27] A. Sarkar, R.G. Ghanem, Mid-frequency structural dynamics with parameter uncertainty, *Computational Methods in Applied Mathematics* 191 (2002) 5499–5513.
[28] C. Semler, W.C. Gentleman, M. Païdoussis, Numerical solutions of second order implict non-linear ordinary differential equations, *Journal of Sound and Vibration* 195 (4) (1996) 553–574.
[29] W. Schoutens, *Stochastic Processes and Orthogonal Polynomials*, Springer, New York, 2000.
[30] B.H.K. Lee, L.Y. Jiang, Y.S. Wong, Flutter of an airfoil with a cubic nonlinear restoring force, *39th AIAA/ASME/ASCE/AHS/ASC Structures, Structural Dynamics, and Materials Conference*, Long Beach, CA, 1998, AIAA-1998-1725.
[31] R.T. Jones, The unsteady lift of a wing of finite aspect ratio, NACA Report 681, 1940.
[32] B.H.K. Lee, P. LeBlanc, Flutter analysis of a two-dimensional airfoil with cubic nonlinear restoring force, National Research Council of Canada, NAE-AN-36, NRC 25438, 1986.
[33] J.M.T. Thompson, H.B. Stewart, *Nonlinear Dynamics and Chaos*, John Wiley, Chichester, 1986.
[34] S.T. Ariaratnam, Some illustrative examples of stochastic bifurcations, in: J.M.T. Thompson, S.R. Bishop (Eds.), *Nonlinearity and Chaos in Engineering Dynamics*, Wiley, Chichester, UK, 1994, pp. 267–274.
[35] D. Poirel, S.J. Price, Bifurcation characteristics of a two-dimensional structurally nonlinear airfoil in turbulent flow, *Nonlinear Dynamics* 48 (4) (2007) 423–435.
[36] J.D. Anderson, *Fundamentals of Aerodynamics*, McGraw-Hill, New York, 1991.